INORGANIC CHEMISTRY FRONTIERS

RESEARCH ARTICLE

View Article Online
View Journal | View Issue

Cite this: *Inorg. Chem. Front.*, 2025, **12**, 8776

Excitation energy funnelling in NIR-emissive [YbPrYb] heterometallic complexes

Salauat Kiraev,[a] Diamantoula Maniaki,[b,c] Annika Sickinger,[a] Leoní A. Barrios,[b,c] David Aguilà,[b,c] Olivier Roubeau,[d] Yannick Guyot,[e] Olivier Maury,[a] Laura Abad Galán *[f] and Guillem Aromí *[b,c]

Energy transfer (ET) among different lanthanide ions is a promising avenue to enhance the numerous applications of this photophysical phenomenon, as has been demonstrated in various solid-state materials. It is far less common to observe these phenomena in discrete species containing different lanthanide ions at predetermined locations within their molecular structures. The advantages of this are many, such as the ability to investigate these phenomena with ultimate atomic control, even in solution. A site-selective molecular scaffold combining the ligands H_2LA and H_2LB has been developed to enable the targeted positioning of lanthanide ions based on differences in ionic radii. This architecture allows a Pr^{3+} ion to be stabilised in the central coordination cavity, while smaller Yb^{3+} ions preferentially occupy peripheral sites, giving rise to a [YbPrYb] topology within a discrete heterometallic complex. The resulting compound, $[Yb_2Pr(LA)_2(LB)_2(H_2O)_2(py)]NO_3$, has been structurally characterised and used to investigate intramolecular ET between Pr^{3+} and Yb^{3+} ions. Two structural analogues, [YbLaYb] and [LuPrLu], were employed as luminescence controls to independently probe the donor and acceptor roles of each metal ion. Photophysical studies in solution and in the solid state revealed two distinct ET processes: a highly efficient $Pr^{3+} \rightarrow Yb^{3+}$ transfer, resulting in near-infrared (NIR) emission at 980 nm, and a competitive $Yb^{3+} \rightarrow Pr^{3+}$ back-transfer, leading to non-radiative deactivation. Lifetime analyses confirmed that both transfer pathways occur with near-quantitative efficiency. These findings represent the first evidence of bidirectional $Pr^{3+} \rightleftarrows Yb^{3+}$ energy transfer within a molecular complex and highlight the power of ligand architecture in enabling and modulating lanthanide photophysical behaviour.

Received 28th July 2025,
Accepted 2nd October 2025

DOI: 10.1039/d5qi01585e

rsc.li/frontiers-inorganic

Introduction

The unique photophysical behaviour of trivalent lanthanide ions arises from their shielded 4f orbitals, which give rise to a cascade of long-lived excited states and narrow emission bands spanning from the ultraviolet to the near-infrared (NIR) region.[1] These transitions are parity-forbidden, and often spin-forbidden, resulting in low absorption coefficients but long radiative lifetimes. These features render lanthanide ions central to applications in optical telecommunications, bioimaging, solid-state lighting, and solar energy conversion.[2,3] As direct 4f–4f excitation is often inefficient, energy transfer (ET) processes are widely employed to sensitise their luminescence. These processes typically involve the excitation of a chromophore or another metal ion, followed by non-radiative energy transfer to the lanthanide acceptor with eventual photon emission from the lanthanide excited state.

Sensitisation through ligand-to-metal ET is well established, particularly using π-conjugated organic antennae *via* intersystem crossing (ISC) mechanisms.[4,5] A powerful alternative involves lanthanide-to-lanthanide (Ln → Ln′) energy transfer, which enables the design of up- or down-conversion systems.[6] These multistep processes facilitate access to optical transitions that are otherwise difficult to achieve *via* direct excitation. Up-conversion (UC) is particularly attractive for generating high-energy emission from low-energy photons—relevant to NIR-to-visible imaging and photonic devices.[7] Conversely, down-conversion (DC), or quantum cutting (QC), entails the redistribution of energy from one high-energy photon into two or more low-energy photons, with the potential to exceed

[a]*Univ. Lyon, Institut Lumière Matière, UMR 5306 CNRS–Université Claude Bernard, Lyon 1, 10 rue Ada Byron, F-69622 Villeurbanne Cedex, France*
[b]*Departament de Química Inorgànica i Orgànica, Universitat de Barcelona, Diagonal 645, 08028 Barcelona, Spain. E-mail: aromi@ub.edu*
[c]*Institute of Nanoscience and Nanotechnology of the University of Barcelona (IN2UB), Barcelona, Spain*
[d]*Instituto de Nanociencia y Materiales de Aragón (INMA), CSIC and Universidad de Zaragoza, Plaza San Francisco s/n, 50009 Zaragoza, Spain*
[e]*Univ Lyon, ENS Lyon, CNRS, UMR 5182, Laboratoire de Chimie, F69342 Lyon, France*
[f]*Departamento de Química Inorgánica, Universidad Complutense de Madrid, Avda. Complutense s/n, 28040 Madrid, Spain. E-mail: laabad03@ucm.es*

100% quantum yield and find application in next-generation photovoltaics.[8–10]

Much of the current understanding of Ln → Ln′ ET processes derives from studies on inorganic hosts such as glasses and ceramics, with only a few studies covering up-converting molecular systems, most notably those from the groups of Piguet, Nonat, and Charbonnière,[11–16] including the remarkable Yb^{3+} cooperative luminescence.[17,18] Recently, we have focused on gaining a deeper understanding of Ln → Ln′ ET in heteropolymetallic systems. In this context, we previously reported Nd → Yb ET leading to enhanced Yb^{3+} emission,[19] as well as a detrimental Nd → Er → Nd back transfer leading to luminescence quenching.[20]

In this context, we decided to explore another f-element couple: Pr^{3+}/Yb^{3+}. Our motivation comes from a survey of the inorganic literature where cooperative sensitisation from Pr^{3+} to Yb^{3+} has often been reported in glass matrices. In particular, QC properties were described, where excitation of Pr^{3+} at visible wavelengths results in emission from Yb^{3+} in the NIR.[21–24] However, the energy transfer process for this Pr^{3+}/Yb^{3+} pair is still controversial with different mechanisms proposed. For example, the two-step sequential ET mechanism was first reported by Van der Ende *et al.* (Pr^{3+}: $^3P_0 \rightarrow {}^1G_4$ to Yb^{3+}: $^2F_{5/2} \rightarrow {}^2F_{7/2}$ and Pr^{3+}: $^1G_4 \rightarrow {}^3H_4$ to Yb^{3+}: $^2F_{5/2} \rightarrow {}^2F_{7/2}$),[25,26] the one-step ET mechanism was reported by Van Wijngaarden *et al.*,[26] or an experimentally evidenced cooperative ET process.[27,28] Of particular relevance to this study is a process leading to one IR photon emission at 980 nm for each photon absorbed at 586 nm (resonant with the $^1D_2$ level of Pr^{3+}).[29,30] Notably, despite the promising match of this ET pair, $Pr^{3+} \rightarrow Yb^{3+}$ energy transfer remains virtually unexplored in molecular systems, probably because of the lack of suitable systems to undergo this study. Thus, to the best of our knowledge, no reports to date have demonstrated this energy transfer pathway in discrete coordination compounds.

This gap is both striking and compelling. Molecular lanthanide complexes offer advantages over extended solids: the modularity of synthetic design, the ability to tune donor–acceptor distances, control over metal coordination environments, and the integration of additional functional units into a single scaffold. Nevertheless, the realisation of heterometallic complexes capable of selective Ln–Ln′ energy transfer presents significant synthetic challenges. The similarity in coordination chemistry across the lanthanide series often impedes site-selective metal placement. Achieving this selectivity requires precise control over ligand architecture to favour the formation of non-statistical, pure heterometallic species.

Building on our previous success in developing ligand systems capable of enforcing site-selective binding in [LnLn′][31–33] and [LnLn′Ln][20,34–36] complexes with well-defined topologies, we now explore Pr^{3+} to Yb^{3+} energy transfer within a trinuclear molecular architecture. Our strategy involves a tailored bis-diketonate/dipicolinate ligand system that yields robust, high-purity heterometallic complexes by exploiting the differences in ionic radii among the lanthanides. This enables us to construct [YbPrYb] molecules, in which the central Pr^{3+} ion is flanked by two Yb^{3+} acceptors—an arrangement that offers potential for cooperative energy transfer pathways and enhanced emission efficiency in the NIR region.

Herein, we present the synthesis, structural characterisation, and photophysical investigation of a new $[Yb_2Pr(LA)_2(LB)_2(H_2O)_2(py)]NO_3$ complex, [YbPrYb] (**3**) (H_2LA, 2,6-bis[(3-oxo-3-naphthalene-2yl)propionyl]pyridine; H_2LB, 6-(3-(naphthalene-2-yl)-3-oxopropanoyl)picolinic acid; Fig. 1). This compound serves as a rare molecular platform for studying Pr^{3+}-to-Yb^{3+} energy transfer. Its analogues, [YbLaYb] (**1**)[19] and [LuPrLu] (**2**), are also prepared as luminescence controls (**2** reported here for the first time), permitting discrimination of donor and acceptor contributions and enabling a detailed mechanistic study of the energy transfer pathway.

Notably, the inclusion of an emissive Pr^{3+} complex in solution is particularly significant, as studies on the photoluminescence of praseodymium compounds in molecular environments remain scarce and are typically limited to steady-state emission analyses.[37–40] It is worth noting that Pr^{3+} is special as a lanthanide ion, as it possesses three potentially emissive levels, namely, $^3P_0$ (~21 400 cm^{-1}), $^1D_2$ (~16 900 cm^{-1}), and $^1G_4$ (~14 500 cm^{-1}) (Fig. 2).[41] The emission properties strongly depend on which excited state is populated. In inorganic solids, the $^3P_0$ state is generally populated *via* direct f–f excitation, while in molecular systems, sensitised luminescence generally occurs from the $^1D_2$ state.[42,43] The $^1G_4$ state, on the other hand, is often poorly emissive due to its small energy gap with the $^3F_{4,3}$ states (~1100 cm^{-1}), making multiphonon deactivation processes highly favourable. The ability to probe both the steady-state and time-resolved behaviour of Pr^{3+} emission thus offers valuable insight into its sen-

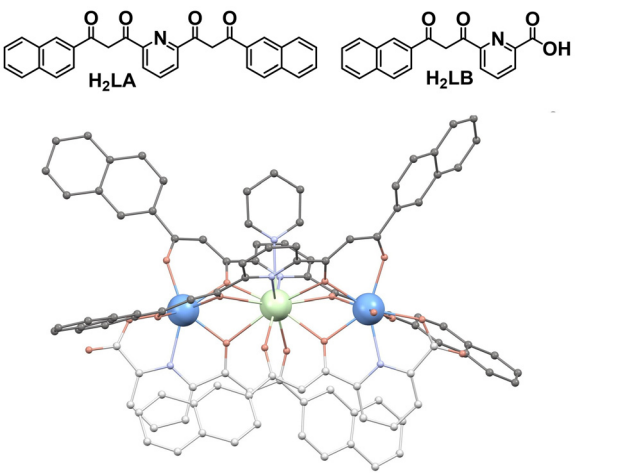

Fig. 1 (Top) Ligands 2,6-bis-((3-oxo-3-naphthalen-2-yl)propionyl)pyridine (H_2LA) and 6-(3-(naphthalen-2-yl)-3-oxopropanoyl)-picolinic acid (H_2LB). (Bottom) Molecular structures of the isostructural cations $[Lu_2Pr(LA)_2(LB)_2(H_2O)_2(py)]^+$ and $[Yb_2Pr(LA)_2(LB)_2(H_2O)_2(py)]^+$ of **2** and **3**. The carbon atoms of ligands LA^{2-} and LB^{2-} are shown in darker and lighter grey, respectively. Lu or Yb is indicated by blue, Pr is indicated by green, O is indicated by salmon colour and N is indicated by purple. H atoms are not shown.

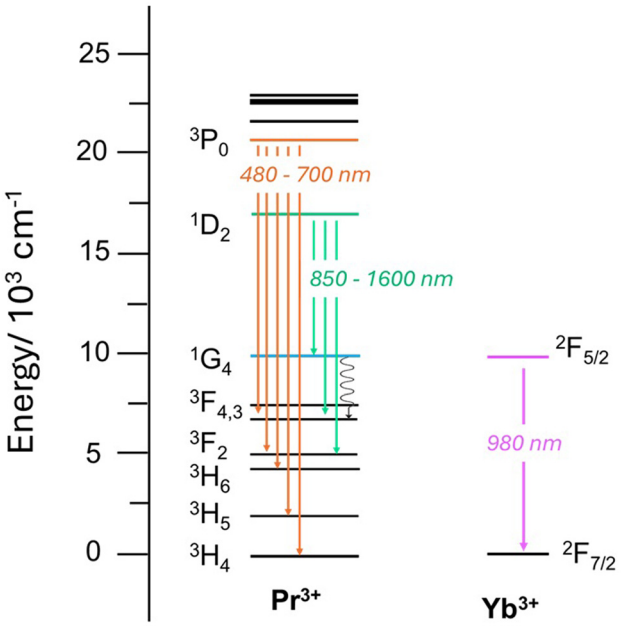

Fig. 2 Simplified energy levels of Pr^{3+} and Yb^{3+}, where the emissive excited states are highlighted in bold along with their corresponding principal radiative transitions.

sitisation and deactivation mechanisms, expanding our understanding of lanthanide photophysics in molecular systems.

Results and discussion

Synthesis and structures

The synergy between the photophysical properties of Pr^{3+} and Yb^{3+} within a molecule was studied on the new heterolanthanide coordination complex $[Yb_2Pr(LA)_2(LB)_2(H_2O)_2(py)]NO_3$, [YbPrYb] (**3**). It was obtained by exploiting a synthetic protocol that enables the generation of very pure and selective [LnLn′Ln] heterometallic molecules by combining stoichiometric amounts of ligands H_2LA[44] and H_2LB[34] with the corresponding amounts of specific Ln^{3+} and Ln'^{3+} salts featuring different ionic radii ($r_{(Ln')} > r_{(Ln)}$).[20,34–36] A balanced chemical equation describing the formation of **3** may be proposed (eqn (1)), albeit the yield of crystals is only about 15%.

$$2Yb(NO_3)_3 + Pr(NO_3)_3 + 2H_2LA + 2H_2LB + 2H_2O + 9py \rightarrow [Yb_2Nd(LA)_2(LB)_2(H_2O)_2(py)]NO_3 + 8HpyNO_3 \quad (1)$$

Compound **2**, $[Lu_2Pr(LA)_2(LB)_2(H_2O)_2(py)]NO_3$, [LuPrLu] was obtained here for the first time in the same manner and with a very similar yield. Homogeneous phases of crystals of **2** or **3** were only obtained by adding one equivalent of $CuCl_2$ to the reaction mixture, which does not participate in the reaction but plays the role of a modulator of crystallisation (see the SI for details).[35] The molecular formulae and structures of **2** and **3** are equivalent as established by single crystal X-ray diffraction (see below). The atomic composition of the bulk crystalline samples of both compounds was established by C, H and N microanalysis and inductively coupled plasma (ICP) metal content determinations, the latter establishing the expected Ln/Ln′ molar ratio within the experimental error (see the SI). For both compounds, this formulation was consistent with the analysis of variable temperature magnetic susceptibility and isothermal field-dependent magnetisation measurements (see the SI and Fig. S1 for details). These experiments confirmed the presence of one Pr^{3+} ion (**2**) or two Yb^{3+} ions only very weakly interacting with a Pr^{3+} centre (**3**), within the respective molecules, considering their experimentally established molecular masses.

Mass spectrometry proved to be a highly valuable technique to corroborate the persistence of the triatomic [LnLn′Ln] assemblies in solution, the purity of the heterometallic 1 : 2 composition and the absence of any metal scrambling. Thus, for both compounds, all fragments composed of three metal ions exhibit the expected composition (Fig. S2–S7), while no equivalent fragments with any other metal distribution were detected. The absence of any metal scrambling is very striking, considering that it is a very common occurrence among lanthanide coordination complexes.[45] This could be explained by a combination of thermodynamic reasons (as previously established through DFT calculations)[36] and the presence of a kinetic barrier that results from the very compact scaffold formed by the $[Ln_2Ln'(LA)_2(LB)_2]^+$ assembly.

The molecular structures of **2** and **3** were determined by SCXRD at 100 K (Tables S1–S3). Both compounds are isostructural; therefore, their structures will be described jointly. The space group is triclinic $P\bar{1}$. The unit cell contains two asymmetric units. The latter is composed of the main complex cation and its NO_3^- counterion, in addition to ten molecules of pyridine of crystallisation. The main complex consists of a trinuclear [LnLn′Ln] coordination molecular array (Fig. 1, and S8–S10; [LuPrLu], **2** and [YbPrYb], **3**) where the metals are coordinated and also bridged by a total of two μ_3-LA^{2-} and two μ-LB^{2-} ligands. The ligands engage all their β-diketonate and dipicolinate-like coordination pockets to chelate the metals, while linking them *via* monoatomic bridges with some of the oxygen atoms in these chelating units. In this manner, the central Pr^{3+} ion is bound to two O,N,O and two O,O coordination pockets and to one terminal pyridine ligand, featuring a coordination number (CN) of 11. The peripheral ions (Lu^{3+} or Yb^{3+}) are surrounded by one O,N,O and two O,O pockets, in addition to one H_2O ligand, exhibiting CN = 8. According to continuous symmetry measures with the program SHAPE,[46] the ideal polyhedra that best describe the central and the side metal positions are a capped pentagonal antiprism and a biaugmented trigonal prism, respectively. The distances (on a 0–100 scale) of Pr^{3+} from its closest ideal geometry are 6.188 and 6.245 for **2** and **3**, respectively, whereas for Lu^{3+} or Yb^{3+}, these separations are 1.514/1.318 and 1.462/1.363, respectively (in the Ln1/Ln2 format). As explained above, the topological selectivity of the [LnLn′Ln] compounds for different lanthanides within the molecule is based on differences in atomic

radii, with the central position hosting the larger metal ions. Here, the average Ln–O bond distances in **2** are 2.644 and 2.303/2.309 Å for Pr and Lu1/Lu2, respectively, while for **3**, these values are 2.646 and 2.311/2.320 Å for Pr and Yb1/Yb2, respectively. Within the complex, the Ln–Pr–Ln angle is 174.45° (Ln═Lu, **2**) and 174.42° (Ln═Yb, **3**); the Ln···Ln distance is 7.837/7.853 Å (for **2**/**3**), while the Pr···Ln separations are 3.924 and 3.922 Å (for **2**) and 3.932 and 3.931 Å (for **3**). Interestingly, the shortest intermolecular Ln···Ln distances are 6.055/6.072 Å (for **2**/**3**); thus, some of these two peripheral metals are closer when lying in two different molecules than when within the same complex. These close intermolecular contacts occur between pairs of complexes that are related by an inversion centre. Each pair is connected by two identical, complementary O–H···O hydrogen bonds, where the water ligand of one molecule forms a hydrogen bond with the oxygen atom of a carboxylate group on the other molecule (Fig. S9 and Table S3).

Photophysical properties

To gain insight into the intramolecular $Pr^{3+} \rightarrow Yb^{3+}$ energy transfer process occurring within the [YbPrYb] (**3**) complex, comparative photophysical studies were carried out using two structurally related analogues: the previously reported [YbLaYb] (**1**)[19] and the newly synthesised [LuPrLu] (**2**) complexes. These were selected to independently probe the roles of the donor and acceptor ions, as complex **1** displays only Yb^{3+} emission at 980 nm, while complex **2** is expected to exhibit luminescence solely from the excited states of Pr^{3+}. All measurements were conducted in dilute (10^{-4} M) 1 : 1 mixtures of MeOH-d_4 and DMSO-d_6 to minimise intermolecular energy transfer events, both at room temperature (RT) and at 77 K. Solid-state measurements were also performed to confirm that the behaviour in solution mirrors the structural features identified by single-crystal X-ray diffraction analysis (Table S4). A summary of the key photophysical parameters obtained from the solution measurements is presented in Table 1.

The triplet excited states of the ligands employed in these systems, H_2LA and H_2LB, have previously been estimated at approximately 18 950 cm^{-1} and 19 050 cm^{-1}, respectively.[19] These energies have been shown to be sufficiently high to enable energy transfer to Yb^{3+} centres, with the $F_{5/2}$ state lying at approximately 10 300 cm^{-1}.[19] In the case of Pr^{3+}, these antennae are expected to sensitise primarily the $^1D_2$ excited state, located around 16 900 cm^{-1}, as they are too low in energy to efficiently populate the higher $^3P_0$ state (21 000 cm^{-1}). Based on this, we limit our consideration to a simplified mechanism of $Pr^{3+} \rightarrow Yb^{3+}$ energy transfer—unlike the multiple possible pathways proposed in ceramic materials—wherein each photon exciting the $^1D_2$ state of Pr^{3+} can, through a cross-relaxation process, result in the emission of a single near-infrared photon from Yb^{3+} ($^2F_{5/2} \rightarrow {}^2F_{7/2}$) at 980 nm.

Table 1 Summary of the key photophysical data for complexes **1**, **2**, and **3** in a 1 : 1 mixture of MeOH-d_4 and DMSO-d_6 (10^{-4} M)

		τ_{obs}[b] (μs)		Φ_{ET}[c]		
Compound	λ_{em}[a] (nm)	RT	77 K	Type	RT	77 K
[YbLaYb] (**1**)	980	16	21	—	—	—
[LuPrLu] (**2**)	1020	0.04	0.30	—	—	—
[YbPrYb] (**3**)	980	0.10	0.09	($Yb^{3+} \rightarrow Pr^{3+}$)	0.99	0.99
	—	—	—	($Pr^{3+} \rightarrow Yb^{3+}$)	1.00	1.00

[a] λ_{exc} = 400 nm. [b] λ_{exc} = 400 nm; λ_{em} = 975 nm (**1**, **3**) and 1020 nm (**2**). [c] Calculated following eqn (2).

This hypothesis was first examined by studying the previously reported [YbLaYb] (**1**) complex in deuterated solutions. Consistent with prior observations in non-deuterated conditions,[19] excitation at 400 nm at RT resulted in the characteristic Yb^{3+} emission profile centred at 980 nm, corresponding to the $^2F_{5/2} \rightarrow {}^2F_{7/2}$ transition (Fig. 3a). At 77 K, the emission spectrum became significantly better resolved due to the reduced line broadening and diminished contributions from thermally populated crystal field-excited states (hot bands). Under these conditions, the four expected transitions associated with the Kramers-split $^2F_{7/2}$ ground state were clearly observed, showing the same spectral features as those previously recorded in non-deuterated solution and here in the solid state (Fig. S11). These results highlight the structural robustness of complex **1** both in solution and in the solid state, where the geometry resolved by SCXRD, featuring C_{2v} symmetry around both Yb^{3+} centres, is preserved in solution. Excited state lifetimes were also measured in deuterated solutions at both RT and 77 K, yielding values of 16 and 21 μs, respectively (Fig. S12). These results indicate a clear decrease in phonon-mediated non-radiative relaxation when compared with the value determined at RT in non-deuterated conditions (9 μs).[47]

Complex **2**, [LuPrLu], was then studied in a similar manner to first assess the effectiveness of the antenna effect in populating the Pr^{3+} $^1D_2$ excited state. First, the emission spectra were recorded in deuterated solution at RT and 77 K, revealing emission almost exclusively in the NIR region. The very subtle emission observed in the visible range is attributed to residual fluorescence and/or phosphorescence from the antenna along with a weak, poorly defined emission band at 607 nm that corresponds to the $^1D_2 \rightarrow {}^3H_4$ transition of Pr^{3+} (Fig. S13). This is not surprising, as the most prominent visible emission of Pr^{3+} results from higher-lying excited states ($^3P_0$) as has been well evidenced in the literature[37,39,40,48–50]

Nonetheless, examples of Pr^{3+} complexes exhibiting NIR emission remain relatively scarce in the literature, underscoring the significance of the results presented here and demonstrating the versatility and efficiency of the antenna system employed. Upon careful analysis of the 77 K emission spectrum, three distinct emission lines can be assigned to the expected transitions originating from the $^1D_2$ excited state, namely, $^1D_2 \rightarrow {}^2F_2$ at 861 nm, $^1D_2 \rightarrow {}^2F_{3,4}$ centred at 1022 nm, and $^1D_2 \rightarrow {}^1G_4$ centred at 1480 nm (Fig. 3b) in agreement with the previously reported NIR-emissive Pr^{3+} complexes.[42,51–53]

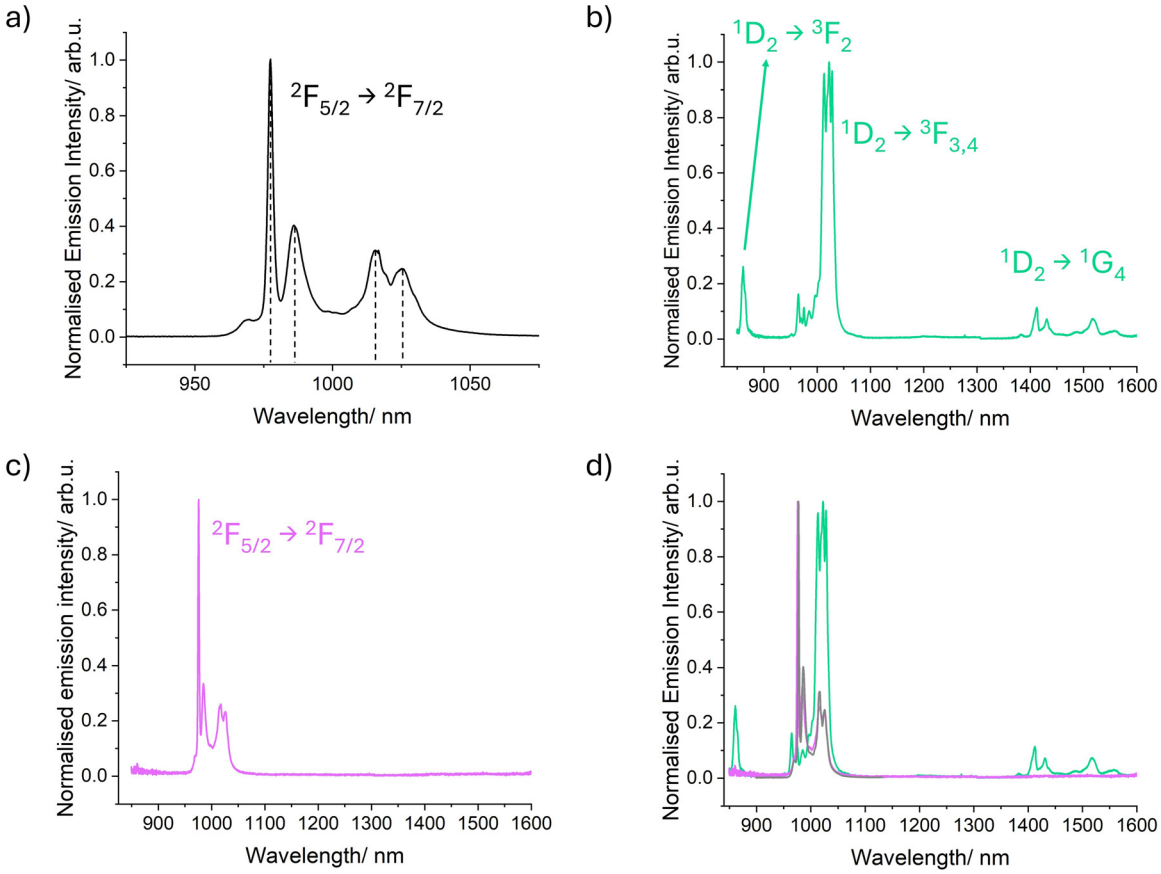

Fig. 3 Emission spectra (λ_{exc} = 400 nm) of complex **1** (black line) (a), complex **2** (green line) (b), complex **3** (pink line) (c), and the comparison of the three (d) in a diluted (10^{-4} M) 1 : 1 mixture of MeOD-d_4 and DMSO-d_6 at 77 K. The dotted lines in (a) denote the crystal field splitting into four Kramers doublets.

As with complex **1**, the emission of complex **2** was further tested in the solid state at 77 K confirming that the structure is preserved upon dissolution (Fig. S14). Finally, the excited-state lifetimes were measured and fitted monoexponentially, giving values of 0.03 μs and 0.4 μs at RT and 77 K, respectively. (Fig. S15) These lifetimes are within the typical range for Pr^{3+}-based NIR emitters and further support the occurrence of efficient population of the $^1D_2$ state.[42,51,52]

Thus, after confirming that both the Yb^{3+} ($^2F_{5/2}$) and Pr^{3+} ($^1D_2$) excited states are efficiently sensitised by our ligand scaffold, we proceeded to investigate the intramolecular energy transfer between the two ions in a molecular system combining both metals. To this end, the emission spectra of the [YbPrYb] (**3**) complex were recorded at both RT and 77 K upon excitation at 400 nm. Interestingly, upon detailed analysis, emission was observed exclusively at 980 nm (Fig. 3c), with a spectral profile identical to that of complex **1** (Fig. 3d). This observation unambiguously indicates that the emission arises from the Yb^{3+} $^2F_{5/2} \rightarrow {}^2F_{7/2}$ transition, while no detectable emission from the Pr^{3+} excited states was present. This behaviour suggests that the $^1D_2$ excited state of Pr^{3+} is deactivated through a non-radiative pathway, most likely due to an efficient quantitative energy transfer to the neighbouring Yb^{3+} centres (Fig. 4). These findings are consistent with previous reports on glass matrices, where $Pr^{3+} \rightarrow Yb^{3+}$ energy transfer occurs efficiently *via* a cross-relaxation mechanism (Pr^{3+}: $^1D_2 \rightarrow {}^3F_4$; Yb^{3+}: $^2F_{7/2} \rightarrow {}^2F_{5/2}$), followed by NIR photon emission from Yb^{3+} ($^2F_{5/2} \rightarrow {}^2F_{7/2}$).[29,30] The excited-state lifetime of complex **3** was then measured at 980 nm, yielding values of 0.10 μs at room temperature and 0.09 μs at 77 K after monoexponential fitting (Fig. S16). When comparing these values to those previously measured for complex **1**, a marked shortening of the Yb^{3+} excited-state lifetime is observed. Given that both the ligand scaffold and the geometry around the Yb^{3+} centres are identical in the two complexes, this difference strongly suggests the occurrence of an additional non-radiative deexcitation pathway for the Yb^{3+} excited state, typically a back energy transfer from Yb^{3+} to Pr^{3+}, which is subsequently deactivated *via* non-radiative decay. The efficiency of the suggested $Yb^{3+} \rightarrow Pr^{3+}$ energy transfer can be estimated using the following expression:

$$\Phi_{ET} = 1 - \frac{\tau_q}{\tau_u} \quad (2)$$

where τ_q is the excited-state lifetime of Yb^{3+} in the presence of Pr^{3+} (**3**) and τ_u is the lifetime in the absence of Pr^{3+} (**1**). Using

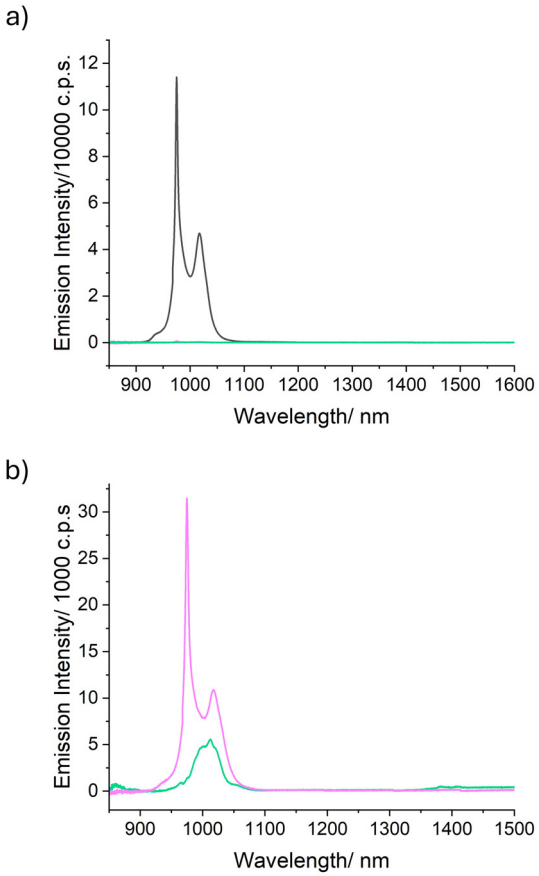

Fig. 4 Emission spectra (λ_{exc} = 400 nm) of complex **1** (black line), complex **2** (green line), and complex **3** (pink line) in an iso-absorbance diluted (10^{-4} M) 1 : 1 mixture of MeOH-d_4 and DMSO-d_6 at RT (a) and a zoomed view of complexes **2** and **3** (b).

the measured lifetimes at 980 nm, this yields an energy transfer efficiency of Φ_{ET} = 0.99, indicating an almost quantitative transfer from Yb^{3+} to Pr^{3+}. This process has also been proposed in solid-state systems, where a clear quenching of Yb^{3+} emission is observed upon increasing the Pr^{3+} concentration.[54] However, to our knowledge, such behaviour has never been demonstrated in discrete molecular systems.

To further probe the occurrence of this dual-path energy transfer between the lanthanide centres, iso-absorbance diluted solutions (OD = 0.56 at 400 nm, Fig. S17) of complexes **1**, **2**, and **3** were studied under identical photophysical conditions at room temperature, allowing direct comparison of their emission intensities (Fig. 4). It is immediately evident that the emission of complex **1** at 980 nm is more intense than that of complexes **2** and **3** (Fig. 4a). Therefore, to better resolve the differences between complexes **2** and **3**, a separate photophysical comparison was carried out (Fig. 4b). Upon moving from complex **2** to complex **3**, the Pr^{3+} emission vanished, while a distinct Yb^{3+} emission at 980 nm emerged, clearly confirming efficient $Pr^{3+} \rightarrow Yb^{3+}$ energy transfer. However, when comparing this to the emission of complex **1**, a marked decrease in intensity is observed, supporting the occurrence of a back-energy transfer $Yb^{3+} \rightarrow Pr^{3+}$, which is subsequently deactivated non-radiatively. We investigated the possible origin of this energy transfer by comparing the absorption spectrum of Pr^{3+} (here measured on the salt $PrCl_3{\cdot}6H_2O$) with the Yb^{3+} emission in complex **1** (Fig. S18). This comparison shows that a clear spectral overlap occurs in the NIR between the Yb^{3+} $^2F_{5/2} \rightarrow {}^2F_{7/2}$ emission band and the Pr^{3+} $^3H_4 \rightarrow {}^1G_4$ absorption band. In the framework of the Förster theory, this spectral overlap strongly suggests a FRET transfer from the Yb^{3+} $^2F_{5/2}$ excited state to the Pr^{3+} $^1G_4$ one, followed by non-radiative deactivation to the Pr^{3+} $^3H_4$ ground state.

Conclusions

A unique combination of ligands capable of stabilising very selectively trinuclear heterometallic lanthanide complexes with a [LnLn′Ln] linear core ($r_{(Ln')} > r_{(Ln)}$) gives access to a topologically pure [YbPrYb] complex. Photophysical investigation of this compound, assisted by comparison with the analogous [YbLaYb] and [LuPrLu] complexes, demonstrates a dual ET pathway at the molecular level: an efficient forward $Pr^{3+} \rightarrow Yb^{3+}$ process, leading to characteristic Yb^{3+} emission at 980 nm, and a competing back-transfer $Yb^{3+} \rightarrow Pr^{3+}$ pathway, which quenches the Yb^{3+} excited state through non-radiative deactivation (Fig. 5). This bidirectional energy exchange, so far never evidenced in molecular systems for this pair of lanthanide centres, underscores the dynamic nature of lanthanide–lanthanide interactions and the pivotal role of the precise coordination environment of the metals in tuning their photo-

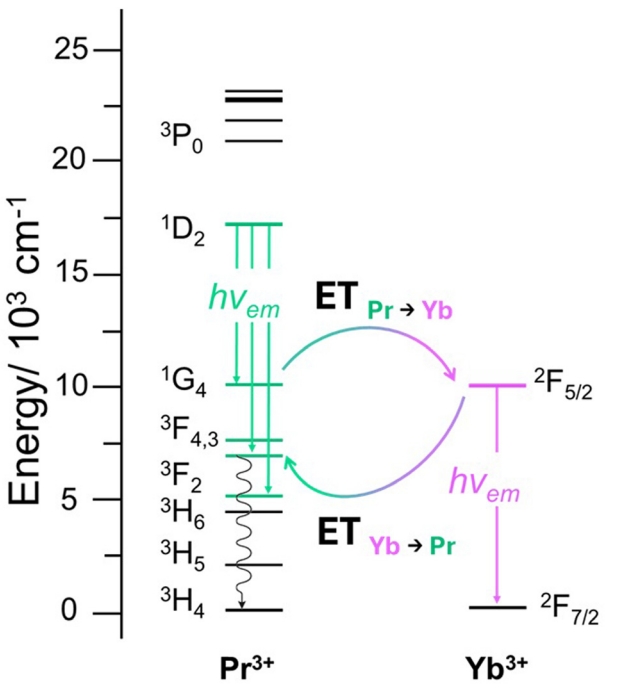

Fig. 5 Energy level diagram schematically showing the proposed energy transfer processes.

physical behaviour. These findings extend current understanding of lanthanide-to-lanthanide ET into the domain of molecular chemistry and offer new strategies for developing solution-processable lanthanide materials for photonics.

Author contributions

S. K.: conceptualization and photophysical data interpretation; D. M.: coordination chemistry synthesis and collection of photophysical data; A. S.: collection of photophysical data and interpretation; L. A. B.: conceptualization, ligand synthesis and coordination chemistry synthesis; D. A.: conceptualization and coordination chemistry synthesis; O. R.: crystal structure determination and magnetic properties; Y. G.: collection of photophysical data and interpretation; O. M.: conceptualization and photophysical data interpretation; L. A. G.: conceptualization, photophysical data interpretation and paper writing; and G. A.: research coordination, conceptualization and paper writing.

Conflicts of interest

There are no conflicts to declare.

Data availability

The data supporting this article have been included as part of the supplementary information (SI). Supplementary information: crystallographic details, information on synthetic procedures, ESI-MS, absorption and emission data, lifetime measurements and fits, NMR experiments, magnetic data treatment, and DFT calculations. See DOI: **https://doi.org/10.1039/d5qi01585e**.

CCDC 2472886 (**3**) and 2472887 (**2**) contain the supplementary crystallographic data for this paper.[55a,b]

Acknowledgements

G. A. thanks the NextGenerationEU/PRTR-C17.I1 (from "Plan Complementario en Comunicación Cuántica" funded by Generalitat de Catalunya and the European Union) and Generalitat de Catalunya for the ICREA Academia 2023 prize. G. A., D. M., L. A. B., D. A. and O. R. thank the Spanish Ministry of Innovation for grants PID2020-118329RB-I00, PID2022-137764OB-I00, PDC2022-133184-I00 and TED2021-129214B-I00. DM thanks the Generalitat de Catalunya for an FI-SDUR Grant (2020-FISDU-00492).

References

1 J.-C. G. Bünzli, On the design of highly luminescent lanthanide complexes, *Coord. Chem. Rev.*, 2015, **293–294**, 19–47.
2 T. Jüstel, H. Nikol and C. Ronda, New developments in the field of luminescent materials for lighting and displays, *Angew. Chem., Int. Ed.*, 1998, **37**, 3084–3103.
3 C. Alexander, Z. Guo, P. B. Glover, S. Faulkner and Z. Pikramenou, Luminescent lanthanides in biorelated applications: From molecules to nanoparticles and diagnostic probes to therapeutics, *Chem. Rev.*, 2025, **125**, 2269–2370.
4 J.-C. G. Bünzli and S. V. Eliseeva, *Basics of Lanthanide Photophysics*, Springer Berlin Heidelberg, 2010, pp. 1–45. DOI: **10.1007/4243_2010_3**.
5 A. D'Aléo, F. Pointillart, L. Ouahab, C. Andraud and O. Maury, Charge transfer excited states sensitization of lanthanide emitting from the visible to the near-infra-red, *Coord. Chem. Rev.*, 2012, **256**, 1604–1620.
6 F. Auzel, Upconversion and anti-Stokes processes with f and d ions in solids, *Chem. Rev.*, 2004, **104**, 139–174.
7 M. Haase and H. Schäfer, Upconverting nanoparticles, *Angew. Chem., Int. Ed.*, 2011, **50**, 5808–5829.
8 Y. Tai, G. Zheng, H. Wang and J. Bai, Broadband down-conversion based near infrared quantum cutting in Eu^{2+}–Yb^{3+} co-doped $SrAl_2O_4$ for crystalline silicon solar cells, *J. Solid State Chem.*, 2015, **226**, 250–254.
9 F. Enrichi, C. Armellini, S. Belmokhtar, A. Bouajaj, A. Chiappini, M. Ferrari, A. Quandt, G. C. Righini, A. Vomiero and L. Zur, Visible to NIR downconversion process in Tb^{3+}–Yb^{3+} codoped silica–hafnia glass and glass–ceramic sol–gel waveguides for solar cells, *J. Lumin.*, 2018, **193**, 44–50.
10 Z. Wang and A. Meijerink, Dye-sensitized downconversion, *J. Phys. Chem. Lett.*, 2018, **9**, 1522–1526.
11 N. Souri, P. Tian, C. Platas-Iglesias, K.-L. Wong, A. Nonat and L. J. Charbonnière, Upconverted photosensitization of Tb visible emission by NIR Yb excitation in discrete supramolecular heteropolynuclear complexes, *J. Am. Chem. Soc.*, 2017, **139**, 1456–1459.
12 L. J. Charbonnière, A. M. Nonat, R. C. Knighton and L. Godec, Upconverting photons at the molecular scale with lanthanide complexes, *Chem. Sci.*, 2024, **15**, 3048–3059.
13 A. Nonat, C. F. Chan, T. Liu, C. Platas-Iglesias, Z. Liu, W.-T. Wong, W.-K. Wong, K.-L. Wong and L. J. Charbonnière, Room temperature molecular up conversion in solution, *Nat. Commun.*, 2016, **7**, 11978.
14 L. Aboshyan-Sorgho, C. Besnard, P. Pattison, K. R. Kittilstved, A. Aebischer, J.-C. G. Bünzli, A. Hauser and C. Piguet, Near-infrared→visible light upconversion in a molecular trinuclear d-f-d complex, *Angew. Chem., Int. Ed.*, 2011, **50**, 4108–4112.
15 D. Zare, Y. Suffren, H. Nozary, A. Hauser and C. Piguet, Controlling lanthanide exchange in triple-stranded helicates: A way to optimize molecular light-upconversion, *Angew. Chem., Int. Ed.*, 2017, **56**, 14612–14617.
16 N. Hamon, L. Godec, S. Sanchez, M. Beyler, L. J. Charbonnière and R. Tripier, Upconversion luminescence with bis–pyclen Yb(III) chelates: Crown vs. linear

polyether linkers in discrete heteropolynuclear architectures, *Angew. Chem., Int. Ed.*, 2025, **64**, e202414608.

17 R. C. Knighton, L. K. Soro, L. Francés-Soriano, A. Rodríguez-Rodríguez, G. Pilet, M. Lenertz, C. Platas-Iglesias, N. Hildebrandt and L. J. Charbonnière, Cooperative luminescence and cooperative sensitisation upconversion of lanthanide complexes in solution, *Angew. Chem., Int. Ed.*, 2022, **61**, e202113114.

18 L. Godec, R. C. Knighton, N. Hamon, W. Thor, K.-L. Wong, R. Tripier and L. J. Charbonnière, Heteropolynuclear lanthanide(III) complexes for cooperative sensitization upconversion in water, *J. Am. Chem. Soc.*, 2025, **147**, 31187–31197.

19 D. Maniaki, A. Sickinger, L. A. Barrios, D. Aguilà, O. Roubeau, N. S. Settineri, Y. Guyot, F. Riobé, O. Maury, L. A. Galán and G. Aromí, Distributive Nd-to-Yb energy transfer within pure [YbNdYb] heterometallic molecules, *Inorg. Chem.*, 2023, **62**, 3106–3115.

20 D. Maniaki, A. Sickinger, L. A. Barrios, D. Aguilà, O. Roubeau, Y. Guyot, F. Riobé, O. Maury, L. Abad Galán and G. Aromí, Energy exchange between Nd^{3+} and Er^{3+} centers within molecular complexes, *Chem. Sci.*, 2024, **15**, 18295–18302.

21 S. Tomar, N. K. Mishra, V. Chauhan, K. Kumar and C. Shivakumara, Study of multimodal light emissions from Pr^{3+}/Yb^{3+} doped $NaLa(MoO_4)_2$ phosphors for optoelectronic devices and plant-growth applications, *Dalton Trans.*, 2025, **54**, 1913–1928.

22 F. E. Maturi, A. Gaddam, C. D. S. Brites, J. M. M. Souza, H. Eckert, S. J. L. Ribeiro, L. D. Carlos and D. Manzani, Extending the palette of luminescent primary thermometers: Yb^{3+}/Pr^{3+} co-doped fluoride phosphate Glasses, *Chem. Mater.*, 2023, **35**, 7229–7238.

23 M. Seshadri, I. T. C. Santos, M. J. V. Bell, J. Lapointe, Y. Messaddeq and V. Anjos, Near-infrared quantum cutting luminescence in Pr^{3+}/Yb^{3+} doped lead bismuth borate glass, *Sci. Rep.*, 2022, **12**, 19311.

24 D. Ding, J. Gao, S. Zhang and L. Duo, The photoluminescence properties of Pr^{3+}-Yb^{3+} co-doped gallo-germanate glasses and glass ceramics as energy converter, *J. Lumin.*, 2020, **226**, 117512.

25 B. M. Van Der Ende, L. Aarts and A. Meijerink, Near-infrared quantum cutting for photovoltaics, *Adv. Mater.*, 2009, **21**, 3073–3077.

26 J. T. van Wijngaarden, S. Scheidelaar, T. J. H. Vlugt, M. F. Reid and A. Meijerink, Energy transfer mechanism for downconversion in the (Pr^{3+}, Yb^{3+}) couple, *Phys. Rev. B: Condens. Matter Mater. Phys.*, 2010, **81**, 155112.

27 S. Balaji, D. Ghosh, K. Biswas, G. Gupta and K. Annapurna, Experimental evidence for quantum cutting co-operative energy transfer process in Pr^{3+}/Yb^{3+} ions co-doped fluorotellurite glass: dispute over energy transfer mechanism, *Phys. Chem. Chem. Phys.*, 2016, **18**, 33115–33125.

28 Y. Katayama and S. Tanabe, Mechanism of quantum cutting in Pr^{3+}–Yb^{3+} codoped oxyfluoride glass ceramics, *J. Lumin.*, 2013, **134**, 825–829.

29 L. J. Borrero-González, G. Galleani, D. Manzani, L. A. O. Nunes and S. J. L. Ribeiro, Visible to infrared energy conversion in Pr^{3+}–Yb^{3+} co-doped fluoroindate glasses, *Opt. Mater.*, 2013, **35**, 2085–2089.

30 Q. J. Chen, W. J. Zhang, X. Y. Huang, G. P. Dong, M. Y. Peng and Q. Y. Zhang, Efficient down- and up-conversion of Pr^{3+}–Yb^{3+} co-doped transparent oxyfluoride glass ceramics, *J. Alloys Compd.*, 2012, **513**, 139–144.

31 D. Aguilà, L. A. Barrios, V. Velasco, O. Roubeau, A. Repollés, P. J. Alonso, J. Sesé, S. J. Teat, F. Luis and G. Aromí, Heterodimetallic [LnLn′] lanthanide complexes: Toward a chemical design of two-qubit molecular spin quantum gates, *J. Am. Chem. Soc.*, 2014, **136**, 14215–14222.

32 J. González-Fabra, N. A. G. Bandeira, V. Velasco, L. A. Barrios, D. Aguilà, S. J. Teat, O. Roubeau, C. Bo and G. Aromí, Thermodynamic stability of heterodimetallic LnLn complexes: Synthesis and DFT studies, *Chem. – Eur. J.*, 2017, **23**, 5117–5125.

33 D. Aguilà, V. Velasco, L. A. Barrios, J. González-Fabra, C. Bo, S. J. Teat, O. Roubeau and G. Aromí, Selective lanthanide distribution within a comprehensive series of heterometallic LnPr complexes, *Inorg. Chem.*, 2018, **57**, 8429–8439.

34 V. Velasco, L. A. Barrios, M. Schütze, O. Roubeau, F. Luis, S. J. Teat, D. Aguilà and G. Aromí, Controlled heterometallic composition in linear trinuclear [LnCeLn] lanthanide molecular assemblies, *Chem. – Eur. J.*, 2019, **25**, 15228–15232.

35 E. Macaluso, M. Rubín, D. Aguilà, A. Chiesa, L. A. Barrios, J. I. Martínez, P. J. Alonso, O. Roubeau, F. Luis, G. Aromí and S. Carretta, A heterometallic [LnLn′Ln] lanthanide complex as a qubit with embedded quantum error correction, *Chem. Sci.*, 2020, **11**, 10337–10343.

36 D. Maniaki, D. Garay-Ruiz, L. A. Barrios, D. O. T. A. Martins, D. Aguilà, F. Tuna, D. Reta, O. Roubeau, C. Bo and G. Aromí, Unparalleled selectivity and electronic structure of heterometallic [LnLn′Ln] molecules as 3-qubit quantum gates, *Chem. Sci.*, 2022, **13**, 5574–5581.

37 A. I. Voloshin, N. M. Shavaleev and V. P. Kazakov, Luminescence of praseodymium(III) chelates from two excited states ($^3P_0$ and $^1D_2$) and its dependence on ligand triplet state energy, *J. Lumin.*, 2001, **93**, 199–204.

38 C. Pettinari, F. Marchetti, R. Pettinari, A. Drozdov, S. Troyanov, A. I. Voloshin and N. M. Shavaleev, Synthesis, structure and luminescence properties of new rare earth metal complexes with 1-phenyl-3-methyl-4-acylpyrazol-5-ones, *J. Chem. Soc., Dalton Trans.*, 2002, 1409, DOI: **10.1039/b108058j**.

39 V. M. Korshunov, M. T. Metlin, S. A. Ambrozevich, I. S. Golovanov, V. E. Gontcharenko, A. S. Selyukov and I. V. Taydakov, Impact of ligand-centered excited states on luminescence sensitization in Pr^{3+} complexes with β-diketones, *Spectrochim. Acta, Part A*, 2021, **260**, 119863.

40 N. Lalioti, E. Zygouri, V. Nastopoulos, N. Panagiotou, C. D. S. Brites, L. D. Carlos, J. Corredoira-Vázquez and

V. Tangoulis, Luminescent thermometer based on a praseodymium(III) cyanide-based metal–organic framework, *Inorg. Chem.*, 2025, **64**, 192–201.

41 W. T. Carnall, G. L. Goodman, K. Rajnak and R. S. Rana, A systematic analysis of the spectra of the lanthanides doped into single crystal LaF3, *J. Chem. Phys.*, 1989, **90**, 3443–3457.

42 J. Scholten, G. A. Rosser, J. Wahsner, N. Alzakhem, C. Bischof, F. Stog, A. Beeby and M. Seitz, Anomalous reversal of C–H and C–D quenching efficiencies in luminescent praseodymium cryptates, *J. Am. Chem. Soc.*, 2012, **134**, 13915–13917.

43 A. F. Martins, S. V. Eliseeva, H. F. Carvalho, J. M. C. Teixeira, C. T. B. Paula, P. Hermann, C. Platas-Iglesias, S. Petoud, É. Tóth and C. F. G. C. Geraldes, A bis (pyridine *N*-oxide) analogue of DOTA: Relaxometric properties of the GdIII complex and efficient sensitization of visible and NIR-emitting lanthanide(III) cations including PrIII and HoIII, *Chem. – Eur. J.*, 2014, **20**, 14834–14845.

44 L. A. Barrios, E. Peyrecave-Lleixa, G. A. Craig, O. Roubeau, S. J. Teat and G. Aromí, Unusual crystal packing in a family of Fe{2,6-bis(pyrazol-3-yl)pyridine}(2) (2+) compounds and the effect on the occurrence of spin crossover and its cooperative character, *Eur. J. Inorg. Chem.*, 2014, 6013–6021.

45 M. Rancan, M. Rando, L. Bosi, A. Carlotto, R. Seraglia, J. Tessarolo, S. Carlotto, G. H. Clever and L. Armelao, Dynamic lanthanide exchange between quadruple-stranded cages: The effect of ionic radius differences on kinetics and thermodynamics, *Inorg. Chem. Front.*, 2022, **9**, 4495–4505.

46 P. Alemany, D. Casanova, S. Alvarez, C. Dryzun and D. Avnir, in *Reviews in Computational Chemistry*, 2017, pp. 289–352. DOI: **10.1002/9781119356059.ch7**.

47 E. Kreidt, C. Kruck and M. Seitz, in *Handbook on the Physics and Chemistry of Rare Earths*, ed. J.-C. G. Bünzli and V. K. Pecharsky, Elsevier, 2018, vol. 53, pp. 35–79.

48 H. Youssef, J. Becker, C. Pietzonka, I. V. Taydakov, F. Kraus and K. Müller-Buschbaum, Divalent europium, NIR and variable emission of trivalent Tm, Ho, Pr, Er, Nd, and Ce in 3D frameworks and 2D networks of Ln-pyridylpyrazolates, *Chemistry*, 2023, **5**, 1006–1027.

49 A. B. Ganaie, A. Ali and K. Iftikhar, Synthesis, structure, phase controlled colour tuning of dinuclear Pr(III) and Tb (III) complexes with fluorinated β-diketone and heterocyclic Lewis base as UV light converters, *Polyhedron*, 2022, **212**, 115592.

50 M. T. Metlin, S. A. Ambrozevich, D. A. Metlina, A. G. Vitukhnovsky and I. V. Taydakov, Luminescence of pyrazolic 1,3-diketone Pr^{3+} complex with 1,10-phenanthroline, *J. Lumin.*, 2017, **188**, 365–370.

51 G. M. Davies, R. J. Aarons, G. R. Motson, J. C. Jeffery, H. Adams, S. Faulkner and M. D. Ward, Structural and near-IR photophysical studies on ternary lanthanide complexes containing poly(pyrazolyl)borate and 1,3-diketonate ligands, *Dalton Trans.*, 2004, 1136–1144, DOI: **10.1039/b400992d**.

52 X. Feng, Y. Shang, H. Zhang, R. Li, W. Wang, D. Zhang, L. Wang and Z. Li, Enhanced luminescence and tunable magnetic properties of lanthanide coordination polymers based on fluorine substitution and phenanthroline ligand, *RSC Adv.*, 2019, **9**, 16328–16338.

53 E. G. Moore, G. Szigethy, J. Xu, L.-O. Pålsson, A. Beeby and K. N. Raymond, 3-Hydroxypyridin-2-one complexes of near-infrared (NIR) emitting lanthanides: sensitization of holmium(III) and praseodymium(III) in aqueous solution, *Angew. Chem., Int. Ed.*, 2008, **47**, 9500–9503.

54 R. Wang, C. Tan, H. Hou, H. Wang, B. Zou and R. Zeng, Multimode luminescence and highly anti-thermal quenching in $Sb^3/Yb^3/Pr^3$ Co-doped Cs_2NaYCl_6 double perovskites, *J. Mater. Chem. C*, 2025, **13**, 10072–10079.

55 (*a*) CCDC 2472886: Experimental Crystal Structure Determination, 2025, DOI: **10.5517/ccdc.csd.cc2p07jh**; (*b*) CCDC 2472887: Experimental Crystal Structure Determination, 2025, DOI: **10.5517/ccdc.csd.cc2p07kj**.